Theory for phonon pumping by magnonic spin currents

S. M. Rezende,[1,*] D. S. Maior,[1] O. Alves Santos,[2] and J. Holanda[3]

[1]*Departamento de Física, Universidade Federal de Pernambuco, 50670-901 Recife, PE, Brazil*

[2]*Physics of Nanodevices, Zernike Institute for Advanced Materials, University of Groningen, Nijenborgh 4, Groningen AG 9747, Netherlands*

[3]*Departamento de Física, Universidade Federal do Espírito Santo, 29075-910 Vitória, Espírito Santo, Brazil*

(Received 12 February 2021; accepted 24 March 2021; published 21 April 2021)

In recent years several experimental observations and theoretical predictions of unique phenomena involving the interplay between spin currents and the coupled magnetization-elastic dynamics have invigorated the field of spintronics. One important experiment reported several years ago showed that elastic waves can produce spin pumping, that is, generation of spin currents in a metallic film in contact with a ferromagnetic material. Very recently the Onsager reciprocal of this effect has been observed in samples made of a film of the insulating ferrimagnet yttrium iron garnet in contact with a platinum strip with nanoscopic silver particles that is known to exhibit a giant spin Hall effect. By passing an electric current through the metallic strip, the spin current generated by the spin Hall effect produces a large magnonic spin current that excites phonons with microwave frequency, observed by Brillouin light scattering. Here we show that these experiments are explained by a theory based on a process in which one magnon in the spin current creates one phonon and another magnon, with conservation of energy and momentum. The theoretical value of the critical charge current in the metallic strip necessary to drive phonons and the values of the phonon frequencies are in good agreement with the values measured experimentally.

DOI: 10.1103/PhysRevB.103.144430

I. INTRODUCTION

It has been over a half century since the coupling between spin waves (magnons) and elastic waves (phonons) first attracted the attention of the magnetism community. Magnetoelastic waves, the name given to the coupled spin-elastic waves, with a frequency of a few GHz, were extensively studied in the 1960s in the ferrimagnetic insulator yttrium iron garnet [$Y_3Fe_5O_{12}$(YIG)], a key material for magnon spintronics due to its unique magnetic and elastic properties [1–6]. In recent years, the active field of spintronics has gained additional impetus with the observation or prediction of unique phenomena involving the interplay between spin currents and the coupled magnetization-elastic dynamics, such as spin pumping with elastic waves [7–10], spin wave excitation by elastic waves at magnetic/nonmagnetic interfaces [11,12], sharp structures in the magnetic field dependent spin Seebeck effect due to magnon-phonon momentum-energy matching [13], nonlocal magnon-polaron transport in YIG [14,15], phonon transport controlled by the magnetization dynamics [16–19], direct observation of the magnon-phonon coupling in magnetic insulators by inelastic neutron scattering [20], detection of the phonon spin in magnon-phonon conversion experiments [21], thermoelastic enhancement of the magnonic spin Seebeck effect [22], and other phonon effects in magnon spintronics [23–25]. With damping smaller than in magnons, the utilization of phonons increases the possibilities of using spintronic phenomena in future information and communication technologies.

Very recently, we have reported the observation of phonon pumping by spin currents in a YIG film [26], in a process that is the Onsager reciprocal of the spin pumping by elastic waves, experimentally observed in metallic multilayers [7–10]. The experiments were carried out with crystalline YIG films with thickness in the range 90–160 nm deposited by liquid phase epitaxy on 0.5 mm thick gadolinium-gallium-garnet (GGG) substrates. The spin current is generated in a metallic strip deposited on the YIG film, traversed by an electric current, by means of the spin Hall effect. The metallic strip is made of a platinum layer with nanoscopic silver particles, that exhibits a giant spin Hall effect [27], and the excitations are detected with backscattering Brillouin light scattering (BLS). With zero or small electric current in the metallic strip, the BLS spectra show a thermal magnon peak with frequency that varies with the applied in-plane magnetic field according to the magnon dispersion relation in YIG, as well as field-independent thermal phonon peaks. However, for current intensities larger than a critical value, a very intense peak emerges in the BLS spectrum with frequency different from the ones of the thermal magnon and phonons, and that does not vary with the applied field. This, added to the fact that the frequency of this intense BLS peak is inversely proportional to the thickness of the YIG film, led to the conclusion that the peak is due to phonons pumped by the magnonic spin current in the YIG film, that propagate into the GGG substrate.

In this paper we present a theory for the phonon pumping by magnonic spin currents based on a process in which one magnon in the spin current creates one phonon and another

*sergio.rezende@ufpe.br

magnon, with conservation of energy and momentum. The theoretical value of the critical charge current in the metallic strip necessary to drive phonons is in order of magnitude agreement with the value measured experimentally with Brillouin light scattering by the excited phonons. In Sec. II we review the basic properties of magnons, phonons, and hybrid magnon-phonon excitations. Section III is devoted to the formulation of the theory for phonon pumping by magnons in the magnonic spin current. In Sec. IV we compare the results of the theory with the experimentally measured critical current for phonon pumping and phonon frequency. Finally, Sec. V is devoted to the conclusions.

II. MAGNON-PHONON INTERACTION

We consider a ferromagnetic medium described by a Hamiltonian containing magnetic, elastic, and magnetoelastic contributions. The magnetic part consists of the interactions between individual spins with the magnetic field (Zeeman interaction), the exchange interactions between neighboring spins, and the long-range dipolar interactions. We treat the quantized excitations of the magnetic system with the Holstein-Primakoff approach, which consists of transformations that express the spin operator $\vec{S}_i$ at the lattice site i in terms of boson operators that create or destroy magnons [28,29]. In the first transformation the components of the local spin operator are related to the creation and annihilation operators of spin deviation at site i, denoted respectively by $a_i^\dagger$ and a_i, which satisfy the boson commutation rules $[a_i, a_j^\dagger] = \delta_{ij}$ and $[a_i, a_j] = 0$. Using a coordinate system with $\hat{z}$ along the equilibrium direction of the spins, defining $S_i^+ = S_i^x + iS_i^y$ and $S_i^- = S_i^x - iS_i^y$, it can be shown that the relations that satisfy the commutation rules for the spin components and the boson operators are

$$S_i^+ = (2S)^{1/2}(1 - a_i^\dagger a_i/2S)^{1/2} a_i, \tag{1a}$$

$$S_i^- = (2S)^{1/2} a_i^\dagger (1 - a_i^\dagger a_i/2S)^{1/2}, \tag{1b}$$

$$S_i^z = S - a_i^\dagger a_i, \tag{1c}$$

where S is the spin and $a_i^\dagger a_i \equiv n_i$ is the operator for the number of spin deviations at site i. We will not consider here interactions between magnons, so we use the linear approximation, whereby only the first terms in Eqs. (1a) and (1b) are kept, $S_i^+ \cong (2S)^{1/2} a_i$, $S_i^- \cong (2S)^{1/2} a_i^\dagger$, and $S_i^z = S - a_i^\dagger a_i$. The next step consists in introducing a transformation from the local field operators to collective boson operators $a_k^\dagger$ and a_k, which satisfy the boson commutation rules $[a_k, a_{k'}^\dagger] = \delta_{kk'}$ and $[a_k, a_{k'}] = 0$, considering translational invariance,

$$a_i = N^{-1/2} \sum_k e^{i\vec{k}.\vec{r}_i} a_k, \tag{2}$$

where N is the number of spins in the system and $\vec{k}$ is a wave vector. Due to the presence of the dipolar interaction, it is necessary to introduce a Bogoliubov transformation to diagonalize the full magnon Hamiltonian [29],

$$a_k = u_k c_k - v_k c_{-k}^\dagger, \quad a_{-k}^\dagger = u_{-k} c_{-k}^\dagger - v_{-k}^* c_k, \tag{3}$$

where the two coefficients are given by

$$u_k = \left(\frac{A_k + \omega_k}{2\omega_k}\right)^{1/2}, \quad v_k = \left(\frac{A_k - \omega_k}{2\omega_k}\right)^{1/2}, \tag{4}$$

where

$$\omega_m(k) = \gamma[H + (2zJS/\gamma\hbar)(1 - \gamma_k)]^{1/2} \times [H + (2zJS/\gamma\hbar)(1 - \gamma_k) + 4\pi M \sin^2\theta_k]^{1/2} \tag{5}$$

is the magnon frequency, valid for wavelengths much smaller than the sample dimensions, and the parameter A_k is

$$A_k = g\mu_B H + 2zJS(1 - \gamma_k) + g\mu_B 2\pi M \sin^2\theta_k, \tag{6}$$

where H is the internal static magnetic field, γ is the gyromagnetic ratio ($2\pi \times 2.8$ GHz/kOe for YIG), $4\pi M$ is the saturation magnetization (1.76 kG for YIG at room temperature), θ_k is the angle of the wave vector with the static field, J is the nearest-neighbor exchange interaction constant, z is the number of nearest neighbors, and γ_k is the structure factor, given by

$$\gamma_k = \frac{1}{z} \sum_{\vec{\delta}} e^{i\vec{k}\cdot\vec{\delta}}. \tag{7}$$

For wave numbers smaller than about 10^7 cm^{-1}, $\gamma_k \approx 1 - (ka)^2/z$, where a is the lattice parameter, and Eqs. (5) and (6) can be written approximately as

$$\omega_m(k) = \gamma[H + Dk^2]^{1/2}[H + Dk^2 + 4\pi M \sin^2\theta_k]^{1/2}, \tag{8}$$

$$A_k = \gamma[H + Dk^2 + 2\pi M \sin^2\theta_k], \tag{9}$$

where D is the exchange parameter. Using the transformations (1)–(3) in the spin Hamiltonian one can show that it can be written in a diagonal form representing noninteraction boson particles,

$$\mathcal{H}_m = \sum_k \hbar\omega_m(k) c_k^\dagger c_k, \tag{10}$$

where $\hbar\,\omega_m(k)$ is the energy of a magnon with frequency ω_m and wave vector $\vec{k}$, and $c_k^\dagger$ and c_k are the magnon creation and annihilation operators.

To treat the elastic system, we consider that the ferromagnetic crystal is a continuous solid, elastically isotropic, with average mass density ρ. We also assume that it is a cubic crystal so that, within the linear approximation, the relation between the stress tensor and the strain tensor involves only two different elastic constants, c_{12} and c_{44}. The elastic deformations of the solid are expressed in terms of the vector displacement $\vec{u} = \vec{r} - \vec{r}'$, where $\vec{r}$ is the initial position of an atom or of a volume element, and $\vec{r}'$ is the position after deformation. The contributions of the elastic system to the Hamiltonian arise from the kinetic and potential energies. Introducing the momentum density conjugate to the displacement, $\rho\partial u_i/\partial t$, in the linear approximation the elastic Hamiltonian can be written as [29]

$$\mathcal{H}_e = \int d^3r \left(\frac{\rho}{2}\frac{\partial u_i}{\partial t}\frac{\partial u_i}{\partial t} + \frac{\alpha}{2}\frac{\partial u_i}{\partial x_i}\frac{\partial u_j}{\partial x_j} + \frac{\beta}{2}\frac{\partial u_i}{\partial x_j}\frac{\partial u_i}{\partial x_j}\right), \tag{11}$$

where the elastic constants are written as $\alpha = c_{12} + c_{44}$, $\beta = c_{44}$, for a Cartesian coordinate system chosen with axes lying

along the ⟨100⟩ crystallographic directions. In order to obtain the collective excitation operators for the elastic system, we use the canonical transformation

$$u_i(\vec{r},t)=\left(\frac{\hbar}{V}\right)^{1/2}\sum_{k,\mu}\varepsilon_{i\mu}(\vec{k})Q_k^{\mu}(t)e^{i\vec{k}\cdot\vec{r}}, \tag{12}$$

$$\rho\dot{u}_i(\vec{r},t)=\left(\frac{\hbar}{V}\right)^{1/2}\sum_{k,\mu}\varepsilon_{i\mu}(\vec{k})P_k^{\mu}(t)e^{-i\vec{k}\cdot\vec{r}}, \tag{13}$$

where $\varepsilon_{i\mu}=\hat{x}_i\cdot\hat{\varepsilon}(\vec{k},\mu)$ and $\hat{\varepsilon}(\vec{k},\mu)$ are unitary polarization vectors. We will denote by $\mu=1,2$ the two polarizations transverse to the wave vector $\vec{k}$ and $\mu=3$ the longitudinal one. Notice that from Hermiticity it follows that $Q_k^i=Q_{-k}^{i+}$ and $P_k^i=P_{-k}^{i+}$. The quantization of the elastic vibrations is made through the commutation relations involving $u_i(\vec{r})$ and its conjugate momentum density $\rho\partial\vec{u}/\partial t$. The only noncommuting pair is such that

$$[u_i(\vec{r}),\rho\dot{u}_j(\vec{r}')]=i\hbar\delta_{ij}\delta(\vec{r}-\vec{r}'), \tag{14}$$

which leads to

$$\left[Q_k^{\mu},P_{k'}^{\nu}\right]=i\hbar\delta_{kk'}\delta_{\mu\nu}. \tag{15}$$

In order to diagonalize the elastic Hamiltonian it is necessary to introduce the canonical transformation

$$Q_k^{\mu}=\left[\frac{\hbar}{2\rho\omega_{p\mu}(k)}\right]^{1/2}(b_{\mu-k}^{\dagger}+b_{\mu k}), \tag{16}$$

$$P_k^{\mu}=i\left[\frac{\rho\hbar\omega_{p\mu}(k)}{2}\right]^{1/2}(b_{\mu k}^{\dagger}-b_{\mu-k}), \tag{17}$$

where the new operators satisfy the boson commutation relations,

$$[b_{\mu k},b_{\nu k'}]=0,\quad [b_{\mu k},b_{\nu k'}^{\dagger}]=\delta_{\mu\nu}\delta_{kk'}, \tag{18}$$

and are interpreted as creation and annihilation operators of lattice vibrations, whose quanta are the phonons, and

$$\omega_{p\mu}(k)=k[(\beta+\alpha\delta_{\mu 3})/\rho]^{1/2} \tag{19}$$

is the frequency of phonons with wave number k and polarization μ. With transformations (12)–(17), the Hamiltonian in Eq. (11) becomes

$$\mathcal{H}_e=\sum_{k,\mu}\hbar\omega_{p\mu}(k)(b_{\mu k}^{\dagger}b_{\mu k}+1/2), \tag{20}$$

that represents a system of noninteracting bosons. In terms of the operators in (16) and (17), the displacement and the momentum density operators become

$$u_i=\left(\frac{\hbar}{2\rho V}\right)^{1/2}\sum_{k,\mu}\varepsilon_{i\mu}(\vec{k})\omega_{p\mu}^{-1/2}(b_{\mu k}^{\dagger}e^{-i\vec{k}\cdot\vec{r}}+b_{\mu k}e^{i\vec{k}\cdot\vec{r}}), \tag{21}$$

$$\rho\dot{u}_i=\left(\frac{\rho\hbar}{2V}\right)^{1/2}\sum_{k,\mu}i\varepsilon_{i\mu}(\vec{k})\omega_{p\mu}^{1/2}(b_{\mu k}^{\dagger}e^{i\vec{k}\cdot\vec{r}}-b_{\mu k}e^{-i\vec{k}\cdot\vec{r}}). \tag{22}$$

Due to the spin-orbit interaction, the elastic displacement in a magnetic medium is coupled to the spin excitation. This is what ultimately relaxes the magnetization dynamics in any material and also gives rise to the magnetostrictive properties of ferromagnets. Thus, we expect that if a spin wave has frequency and wave vector close to those of an elastic wave, they become strongly coupled giving rise to hybrid excitations, called magnetoelastic waves, or magnon-phonon hybrid excitations [1–6,29–35].

The magnetoelastic interaction can be expressed by a phenomenological Hamiltonian, which is a function of $\vec{M}$ and $\vec{u}$. For a cubic crystal, with the static field applied along one of the [100] directions, the lowest-order term of the interaction Hamiltonian is given by [29–35]

$$\mathcal{H}_{me}=\int d^3r\frac{b_2}{2}S_iS_j\left(\frac{\partial u_i}{\partial x_j}+\frac{\partial u_j}{\partial x_i}\right), \tag{23}$$

where the repeated indices indicate summation with $i\neq j$, and b_2 is one of the magnetoelastic constants. Using the transformations (1) and (2) and (12)–(17), this Hamiltonian can be written in terms of the magnon and phonon operators. We will assume that the wave vectors of interest lie on the x-z plane of the Cartesian system, and take $\hat{\varepsilon}(\vec{k},1)=\hat{x}$, $\hat{\varepsilon}(\vec{k},2)=\hat{y}$. Neglecting, for simplicity, the transformation (3), i.e., using $u_k=1$ and $v_k=0$, and keeping only components of Eq. (23) quadratic in the boson operators, the magnetoelastic Hamiltonian becomes

$$\begin{aligned}\mathcal{H}_{me}=i\left(\frac{b_2^2\gamma\hbar^2}{4\rho}\right)^{1/2}\sum_k\big[&k\omega_{pt}^{-1/2}\cos 2\theta(c_k+c_{-k}^{\dagger})(b_{1k}^{\dagger}+b_{1-k})\\&-ik\omega_{pt}^{-1/2}\cos\theta(c_k-c_{-k}^{\dagger})(b_{2k}^{\dagger}+b_{2-k})\\&\times-k\omega_{pl}^{-1/2}\sin 2\theta(c_k+c_{-k}^{\dagger})(b_{3k}^{\dagger}+b_{3-k})\big],\end{aligned} \tag{24}$$

where ω_{pt} and ω_{pl} are the shear and longitudinal phonon frequencies. This Hamiltonian reduces to simple forms for waves propagating along ($\theta=0$) or perpendicular ($\theta=\pi/2$) to the magnetic field. For the geometry of interest here, $\theta=\pi/2$, Eq. (24) becomes

$$\mathcal{H}_{me}=-i\left(\frac{b_2^2\gamma\hbar^2}{4\rho}\right)^{1/2}\sum_k k\omega_{pt}^{-1/2}(c_k+c_{-k}^{\dagger})(b_{1k}^{\dagger}+b_{1-k}). \tag{25}$$

Note that longitudinal phonons do not couple with magnons propagating perpendicularly to the magnetic field. Thus, the total Hamiltonian for the magnon-phonon system is

$$\begin{aligned}\mathcal{H}_t=&\sum_k\hbar\omega_m(k)c_k^{\dagger}c_k+\sum_{k,\mu}\hbar\omega_{p\mu}(k)b_{\mu k}^{\dagger}b_{\mu k}\\&-\sum_k i\hbar(\sigma_k/2)(c_k+c_{-k}^{\dagger})(b_{1k}^{\dagger}+b_{1-k}),\end{aligned} \tag{26}$$

where

$$\sigma_k=b_2k\left(\frac{2\gamma}{\rho\omega_{pt}M}\right)^{1/2} \tag{27}$$

is a parameter that expresses the coupling between magnons and phonons, and v_{pt} is the velocity of the transverse phonon, given by $v_{pt}=(c_{44}/\rho)^{1/2}$ for a wave propagating along a [100] axis in a cubic crystal, or $v_{pt}=(\mu_t/\rho)^{1/2}$ in a more general case, where μ_t is the shear modulus. The normal mode frequencies can be calculated using the Heisenberg equation $dA/dt=\partial A/\partial t+(1/i\hbar)[A,\mathcal{H}_t]$ with the Hamiltonian (26).

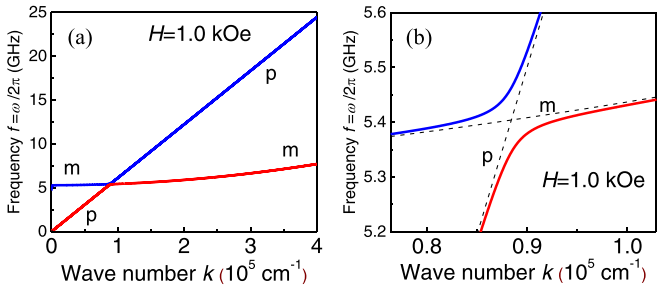

FIG. 1. Magnetoelastic dispersion curves for waves propagating in a YIG film perpendicularly to the static magnetic field with intensity $H = 1.0$ kOe. (a) Full dispersion with two branches. The symbols "m" and "p" indicate the regions where the excitation has almost pure magnon (m) or phonon (p) character. (b) Blowup of the crossover region showing the splitting of the magnetoelastic dispersions (solid lines) and the pure magnon and phonon dispersions (dashed lines).

The equations of motion for the magnon and phonon operators are

$$\frac{dc_k^\dagger}{dt} = i\omega_m c_k^\dagger - \frac{\sigma_k}{2}(b_{1k}^\dagger + b_{1-k}), \tag{28a}$$

$$\frac{db_{1k}^\dagger}{dt} = i\omega_p b_{1k}^\dagger + \frac{\sigma_k}{2}(c_k^\dagger + c_{-k}), \tag{28b}$$

where in Eq. (28), and from now on, ω_p denotes the transverse phonon frequency. In the stationary state, all operators have a $\exp(i\omega t)$ variation, so that, neglecting the coupling between excitations with opposite wave vectors, the magnetoelastic dispersion relation resulting from Eq. (28) is

$$(\omega - \omega_p)(\omega - \omega_m) - (\sigma_k/2)^2 = 0, \tag{29}$$

which is a well-known result [1–6,29–35]. If there is no magnetoelastic coupling, $\sigma_k = 0$ and the roots of Eq. (29) are ω_m and ω_p. Figure 1 shows the dispersion relation, frequency $f = \omega/2\pi$ versus wave number, calculated from the roots of Eq. (29), with the magnon and phonon frequencies of Eqs. (5) and (19) for $\theta = \pi/2$, using the following parameters for YIG: $H = 1.0$ kOe, $4\pi M = 1.76$ kG, $\gamma = 2.8 \times 2\pi \times 10^6\ \mathrm{s^{-1}/Oe}$, $D = 5.4 \times 10^{-9}\ \mathrm{Oe\,cm^2}$, $b_2 = 7.0 \times 10^6\ \mathrm{erg/cm^3}$, $\rho = 5.2\ \mathrm{g/cm^3}$, and $v_p = 3.84 \times 10^5\ \mathrm{cm/s}$. The two branches correspond to the hybridized magnon-linearly polarized phonon. As expected, the magnetoelastic coupling is strongest in the region where the magnon and phonon curves cross, called the crossover region. The zoom of the crossover region in Fig. 1(b) shows that for $H = 1.0$ kOe the magnon and phonon dispersion curves cross at a frequency 5.404 GHz and wave number $k_{cross} = 0.884 \times 10^5\ \mathrm{cm^{-1}}$. It also shows that the frequency splitting is 0.12 GHz, which is quite small compared to the magnon and phonon frequencies.

III. FORMULATION OF THE THEORY FOR PHONON PUMPING

A. Magnon distribution in the magnonic spin current

The theory presented here for the phonon pumping by magnons in the magnonic spin current requires a detailed knowledge of the magnon distribution in the spin current.

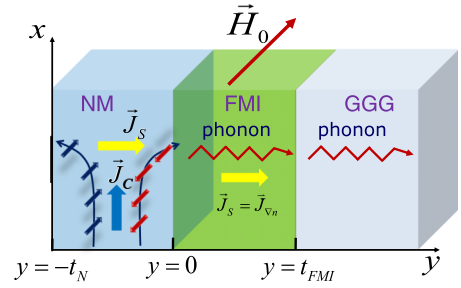

FIG. 2. Illustration of the sample structure used to study the phonon pumping by magnonic spin currents.

Here we calculate the distribution in configuration space and in wave vector space. Consider the structure of the samples used in Ref. [26], consisting of a normal metal (NM)/ferromagnetic insulator (FMI)/GGG substrate, illustrated in Fig. 2, with a charge current in the NM layer with density $\vec{J}_C$. The spin current generated in the NM layer through the spin Hall effect has density [36–40]

$$\vec{J}_S = (\hbar/2e)\theta_{\mathrm{SH}}\hat{\sigma} \times \vec{J}_C, \tag{30}$$

where θ_{SH} is the spin Hall angle. This spin current flows into the FMI layer and creates a magnon accumulation at the interface, that diffuses through the FMI. The spin current in the FMI is carried by spin waves (magnons) in a wide range of wave vectors $\vec{k}$ and energies $\hbar\omega_k$. Call n_k the number of magnons with wave number k in the volume V of the FMI layer, n_k^0 the number in thermal equilibrium, given by the Bose-Einstein distribution,

$$n_k^0 = \frac{1}{e^{\hbar\omega_k/k_BT} - 1}, \tag{31}$$

and

$$\delta n_k = n_k - n_k^0 \tag{32}$$

is the number in excess of equilibrium. The magnon accumulation δn_m is defined as the density of magnons in excess of equilibrium [41,42],

$$\delta n_m(y) = \frac{1}{(2\pi)^3}\int d^3k\big[n_k(y) - n_k^0\big] = \frac{1}{(2\pi)^3}\int d^3k\,\delta n_k. \tag{33}$$

The magnon spin-current density with polarization z, $\vec{J}_S^z$, related to the magnetization current $\vec{J}_M^z$ by $\vec{J}_S^z = \vec{J}_M^z/\gamma$, can be written as

$$\vec{J}_S(y) = \frac{\hbar}{(2\pi)^3}\int d^3k\,\vec{v}_k\big[n_k(y) - n_k^0\big], \tag{34}$$

where $\vec{v}_k$ is the k-magnon velocity. In this equation and from now on, we have omitted the superscript z for simplicity. The spatial distribution of the magnon number under the influence of a gradient can be calculated with the Boltzmann transport equation (BTE). In the absence of external forces and in the relaxation approximation, in steady state BTE gives

$$n_k(y) - n_k^0 = -\tau_k\vec{v}_k \cdot \nabla n_k(y), \tag{35}$$

where τ_k is the k-magnon relaxation time. Using Eq. (35) in Eq. (34) one can show [43,44] that the spin current is the sum of two parts,

$$\vec{J}_S = \vec{J}_{S\nabla T} + \vec{J}_{S\delta n} \tag{36}$$

where

$$\vec{J}_{S\nabla T} = -\frac{\hbar}{(2\pi)^3}\int d^3k\tau_k \frac{\partial n_k^0}{\partial T}\vec{v}_k(\vec{v}_k\cdot\nabla T) \tag{37}$$

is the contribution of the temperature gradient (drift) and

$$\vec{J}_{S\delta n}(y) = -\frac{\hbar}{(2\pi)^3}\int d^3k\tau_k\vec{v}_k[\vec{v}_k\cdot\nabla\delta n_k(y)] \tag{38}$$

is due to the spatial distribution of the magnon accumulation. With Eqs. (36)–(38) one can study the spin Seebeck effect produced by a temperature gradient ∇T applied normal to the plane of the bilayer. Here $\nabla T = 0$, so that we have only the contribution of Eq. (38), that represents a spin current due to spatial variation of the magnon occupation number. This can be written as a diffusion current,

$$J_{S\delta n}(y) = -\hbar D_m\frac{\partial}{\partial y}\delta n_m(y), \tag{39}$$

where D_m is the diffusion parameter, to be calculated. Considering the conservation equation,

$$\frac{\partial}{\partial y}J_{S\delta n}(y) = -\hbar\frac{\delta n_m(y)}{\tau_{mp}}, \tag{40}$$

where τ_{mp} is the time it takes for the magnon system to relax to the phonon temperature, we have in the steady state a diffusion equation for the magnon accumulation,

$$\frac{\partial^2\delta n_m(y)}{\partial y^2} = \frac{\delta n_m(y)}{l_m^2}, \tag{41}$$

where l_m is the diffusion length, related to the diffusion parameter by $D_m = l_m^2/\tau_{mp}$. The solutions of Eq. (41) are

$$\delta n_m(y) = A_1 e^{y/l_m} + A_2 e^{-y/l_m}, \tag{42}$$

which can be written as

$$\delta n_m(y) = A\cosh[(y - t_{\rm FMI})/l_m] + B\sinh[(y - t_{\rm FMI})/l_m], \tag{43}$$

where A and B are coefficients to be determined by the boundary conditions at $y = 0$ and $y = t_{\rm FMI}$. From Eqs. (39) and (43) we have

$$J_{S\delta n}(y) = -\frac{\hbar D_m}{l_m}\{A\sinh[(y - t_{\rm FMI})/l_m] + B\cosh[(y - t_{\rm FMI})/l_m]\}. \tag{44}$$

The boundary conditions are determined by conservation of the angular momentum flow that requires continuity of the spin currents at the interfaces. At the FMI/GGG interface $J_S = 0$, which, with Eq. (44) gives $B = 0$. At $y = 0$ the boundary condition is $J_S(0^-) = J_S(0^+)$. Since in the NM the current density is $J_S(0) = J_S$, we have

$$J_{S\delta n}(y) = -J_S\frac{\sinh[(y - t_{\rm FMI})/l_m]}{\sinh t_{\rm FMI}/l_m}, \tag{45}$$

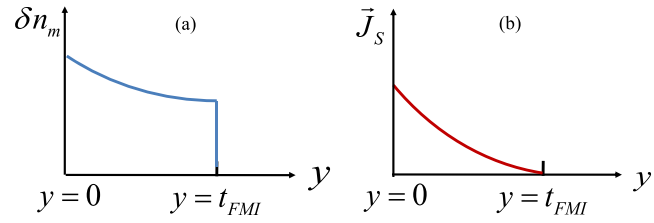

FIG. 3. Variations of the magnon accumulation (a) and spin-current density (b) along the coordinate normal to the sample plane.

so that

$$A = J_S\frac{l_m}{\hbar D_m\sinh(t_{\rm FMI}/l_m)}. \tag{46}$$

Using this result in Eq. (43) we obtain the spatial dependence of the magnon accumulation in the FMI layer produced by the spin current J_S generated in the NM layer,

$$\delta n_m(y) = J_S\frac{l_m}{\hbar D_m\sinh(t_{\rm FMI}/l_m)}\cosh[(y - t_{\rm FMI})/l_m]. \tag{47}$$

The variations of the magnon accumulation and spin-current density along the direction perpendicular to the sample plane are illustrated in Fig. 3. In order to calculate distribution of the magnons in wave vector space we need to find the relevant quantity of the mechanism that drives phonons by the magnonic spin current.

B. Mechanism for phonon pumping by magnons

The mechanism proposed here for the driving of phonons consists of a three-boson process, in which one magnon in the magnonic spin current splits into one phonon and one magnon. The only term in the magnetoelastic Hamiltonian in Eq. (23) that can can lead to a two-magnon one-transverse phonon interaction is

$$\mathcal{H}_{me} \Rightarrow \frac{b_2}{S^2}\int d^3r S_x S_y\frac{\partial u_x}{\partial y}. \tag{48}$$

Using $S_x = (S^+ + S^-)/2$, $S_y = (S^+ - S^-)/2i$, and the transformations (1) to boson operators, Eq. (48) leads to

$$\mathcal{H}_{me} = \frac{b_2}{i2S}\int d^3r(a_i a_i - a_i^\dagger a_i^\dagger)\frac{\partial u_x}{\partial y}. \tag{49}$$

Considering that the wave vector of the phonons detected in the backscattering BLS configuration are perpendicular to the sample plane, with the coordinates in Fig. 2 we have $\vec{k} = k\hat{y}$. Using the transformations from the spin and displacement operators in (1), (2), (12), and (15), Eq. (49) becomes

$$\mathcal{H}_{me} = \frac{b_2}{2SN}\left(\frac{\hbar}{2\rho V}\right)^{1/2}\int d^3r \times\left(\sum_{k,k1,k2} e^{i(\vec{k}_1+\vec{k}_2)\cdot\vec{r}_i}a_{k1}a_{k2} - e^{-i(\vec{k}_1+\vec{k}_2)\cdot\vec{r}_i}a_{k1}^\dagger a_{k2}^\dagger\right) \times k\omega_{tk}^{-1/2}(-b_k^\dagger e^{-iky} + b_k e^{iky}). \tag{50}$$

Clearly, in order to obtain terms in the form $c_{k1}c_{k2}^\dagger$, we have to consider the dipolar interaction and use the Bogoliubov

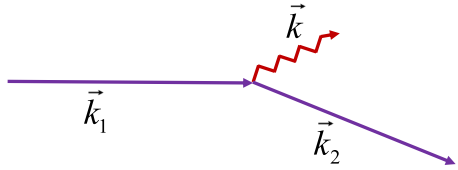

FIG. 4. Illustration of magnon-phonon splitting process in which a magnon with wave vector $\vec{k}_1$ interacts with another magnon $\vec{k}_2$ to generate a phonon with wave vector $\vec{k}$.

transformation (3) that diagonalizes the magnon Hamiltonian. Using the transformations (3) in the Hamiltonian (50) and employing the orthogonality condition

$$\frac{1}{V}\int d^3r \sum_{k'} e^{i(k-k')r} = \delta_{kk'}, \tag{51}$$

we obtain the Hamiltonian for the process by which one magnon undergoes a splitting generating another magnon and one phonon, illustrated in Fig. 4. The magnon-phonon Hamiltonian for this process is

$$\mathcal{H}_{m-p} = \sum_{k_1,k,k_2} (V_{m-p} c_{k1} b_k^\dagger c_{k2}^\dagger + V_{m-p}^* c_{k2}^\dagger b_k c_{k1}) \Delta(\vec{k}_1 - \vec{k} - \vec{k}_2), \tag{52}$$

where

$$V_{m-p} = \frac{b_2}{2SN}\left(\frac{\hbar V}{2\rho}\right)^{1/2} \omega_{pk}^{-1/2} [k_p(u_{k1}v_{k2} + u_{k2}v_{k1}) - k_p(v_{k1}^* u_{k2} + v_{k2}^* u_{k1})].$$

Finally, since k_1, k_2 can be either 1 or 2, and in the last two terms the signs of all ks are the opposite of the first two, we have

$$V_{m-p} = 2\frac{b_2}{SN}\left(\frac{\hbar V}{2\rho}\right)^{1/2} k_p \omega_{pk}^{-1/2} u_{k1} v_{k2}. \tag{53}$$

In this process, a magnon with wave vector $\vec{k}_1$ interacts with another magnon $\vec{k}_2$ to generate a phonon with wave vector $\vec{k}$, by a three-boson splitting process that conserves momentum and energy.

The probability that one phonon in the n_{p_k} mode is created in this process can be calculated with first-order perturbation theory. The matrix element that corresponds to this process is, with the Hamiltonian (52),

$$\langle n_{k1} - 1, n_{pk} + 1, n_{k2} + 1 | \mathcal{H}_{m-p} | n_{k1}, n_{pk}, n_{k2} \rangle = [n_{k1}(n_{pk} + 1)(n_{k2} + 1)]^{1/2} (V_{m-p}).$$

Thus, the probability per unit time for the number of phonons n_{pk} to increase by one unit, given by Fermi's "golden rule," is

$$W_{n_{pk}\to n_{pk}+1} = \frac{2\pi}{\hbar^2} \sum_{k_2} (V_{m-p})^2 [n_{k1}(n_{pk} + 1)(n_{k2} + 1)] \times \delta(\omega_{k1} - \omega_{pk} - \omega_{k2}), \tag{54}$$

where the sum runs only over $\vec{k}_2$ because of the momentum conservation relation $\vec{k}_1 = \vec{k} + \vec{k}_2$. In Eq. (54) and from now on we omit the subscript m in the magnon frequencies to simplify the notation. The reverse process by which the number of phonons decreases by one unit is calculated in a similar manner, so that the time rate of change of the phonon number is given by

$$\frac{dn_{pk}}{dt} = W_{n_{pk}\to n_{pk}+1} - W_{n_{pk}\to n_{pk}-1}. \tag{55}$$

Thus, the rate of change of the number of phonons in mode $\vec{k}$ due to the magnon splitting process is

$$\frac{dn_{pk}}{dt} = \frac{2\pi}{\hbar^2} \sum_{k_2} (V_{m-p})^2 [n_{k1}(n_{pk} + 1)(n_{k2} + 1) - n_{pk} n_{k2}(n_{k1} + 1)] \delta(\omega_{k1} - \omega_{pk} - \omega_{k2}). \tag{56}$$

Introduce the excess in the magnon number of the pumping mode 1, as defined in Eq. (32), and consider that the other magnon mode is in thermal equilibrium, so that

$$\frac{dn_{pk}}{dt} = \frac{2\pi}{\hbar^2} \sum_{k_2} (V_{m-p})^2 [(n_{pk} + 1)(\delta n_{m1} + \bar{n}_{m1})(\bar{n}_{m2} + 1) - n_{pk}\bar{n}_{m2}(\delta n_{m1} + \bar{n}_{m1} + 1)] \delta(\omega), \tag{57}$$

where $\delta(\omega)$ is the delta function as in Eq. (56). This equation can be written as

$$\frac{dn_{pk}}{dt} = \frac{2\pi}{\hbar^2} \sum_{k_2} (V_{m-p})^2 [(n_{pk} + 1)\delta n_{m1} + \delta n_{m1}\bar{n}_{m2} + (n_{pk} + 1)\bar{n}_{m1}(\bar{n}_{m2} + 1) - n_{pk}\bar{n}_{m2}(\bar{n}_{m1} + 1)] \delta(\omega). \tag{58}$$

In thermal equilibrium $dn_{pk}/dt = 0$, so that Eq. (56) gives the following relation for the thermal numbers:

$$(\bar{n}_{pk} + 1)\bar{n}_{m1}(\bar{n}_{m2} + 1) - \bar{n}_{pk}\bar{n}_{m2}(\bar{n}_{m1} + 1) = 0. \tag{59}$$

Actually, this relation follows directly from the expression for the Bose-Einstein distribution, Eq. (31). Adding this null result to Eq. (58) we obtain

$$\frac{dn_{pk}}{dt} = \frac{2\pi}{\hbar^2} \sum_{k_2} (V_{m-p})^2 \big[(n_{pk} + 1)\delta n_{m1} + 2\delta n_{m1}\bar{n}_{m2} + (n_{pk} - \bar{n}_{pk})\bar{n}_{m1}(\bar{n}_{m2} + 1) - \big(n_{pk} - \bar{n}_{p_k}\big)\bar{n}_{m2}(\bar{n}_{m1} + 1)\big] \delta(\omega). \tag{60}$$

If there is no spin-current pumping, $\delta n_{m1} = 0$, so that this equation gives

$$\frac{dn_{pk}}{dt} = -(n_{pk} - \bar{n}_{pk})\frac{2\pi}{\hbar^2} \sum_{k_2} (V_{m-p})^2 \times [\bar{n}_{m2}(\bar{n}_{m1} + 1) - \bar{n}_{m1}(\bar{n}_{m2} + 1)] \delta(\omega), \tag{61}$$

which is consistent with the equation for the relaxation rate due to the three-boson splitting process [29,45]. As will be shown later, the magnons involved in the process have wave numbers on the order of $10^7\,\mathrm{cm}^{-1}$. Hence, since the phonon wave number is on the order of $10^5\,\mathrm{cm}^{-1}$, $k_{m2} = k_{m1} - k_p \approx k_{m1}$. We also consider that the magnon mode population n_{m2} is not perturbed much, so that $n_{m2} \approx \bar{n}_{m2}$. Thus, leaving the

damping term out, Eq. (61) becomes

$$\frac{dn_{pk}}{dt} = n_{pk}\frac{2\pi}{\hbar^2}\sum_{k_m} V_{m-p}^2 \delta n_{mk}\delta(\omega_{mk1} - \omega_{pk} - \omega_{mk2}). \quad (62)$$

This expression can be written in the form

$$\frac{dn_{pk}}{dt} = \alpha_{pk} n_{pk}, \quad (63)$$

where, using Eq. (53) and $M = \gamma\hbar NS/V$, the rate of phonon pumping becomes

$$\alpha_{pk} = 4\pi\frac{\gamma b_2^2 k^2}{MS\rho\omega_{pk}}\frac{1}{N}\sum_{k_m}(u_{mk}v_{mk})^2\delta n_{mk}\delta(\omega_{mk1}-\omega_{pk}-\omega_{mk2}). \quad (64)$$

Replacing the sum by an integral in the Brillouin zone, using

$$\frac{1}{N}\sum_{k} \to \frac{\Omega}{(2\pi)^3}\int d\vec{k}, \quad (65)$$

we have

$$\alpha_{pk} = 4\pi\frac{\gamma b_2^2 k^2}{MS\rho\omega_{pk}}\frac{a^3}{(2\pi)^3}\int d\vec{k}(u_{mk}v_{mk})^2\delta n_{mk} \times \delta(\omega_{mk1} - \omega_{pk} - \omega_{mk2}), \quad (66)$$

that has dimension of time^{-1}, as it should. With Eq. (63) and denoting by η_{pk} the phonon relaxation rate, the equation of motion for the number of pumped phonons is

$$\frac{d(n_{pk} - \bar{n}_{pk})}{dt} = (\alpha_{pk} - \eta_{pk})(n_{pk} - \bar{n}_{pk}), \quad (67)$$

and its solution is

$$n_{pk}(t) - \bar{n}_{pk} = [n_{pk}(0) - \bar{n}_{pk}]e^{(\alpha_{pk}-\eta_{pk})t}. \quad (68)$$

Thus, the critical rate for phonon pumping is given by

$$\alpha_{pk\,cr} = \eta_{pk}. \quad (69)$$

This result shows that phonons can be indeed pumped by the magnon accumulation δn_{mk} in the magnonic spin current, as long as its amplitude is larger than a critical value.

C. Critical current for phonon pumping

In order to calculate the critical current for phonon pumping we need first to calculate the distribution of the relevant magnons in the magnonic spin-current wave vector space. For this we consider for the magnon number a small deviation from the equilibrium distribution in the form $n_k(\vec{r}) = n_k^0 + n_k^0[1 + \lambda_k g(\vec{r})]$, such that λ_k in lowest order of energy is chosen as to eliminate the singularity at $\varepsilon_k = \hbar\omega_k = 0$ [44]. This is

$$n_k(\vec{r}) = n_k^0 + n_k^0\varepsilon_k g(y), \quad (70)$$

where $g(y)$ is a spatial distribution determined by the solution of the boundary-value problem. Substitution in Eq. (33) shows that

$$\delta n_m(y) = I_0 g(y), \quad (71)$$

where $g(y)$ is a function obtained from Eq. (47) and I_0 is a parameter given by the integral

$$I_0 = \frac{1}{(2\pi)^3}\int d^3k n_k^0\varepsilon_k. \quad (72)$$

Using the expansion (7) in Eq. (66), the pumping rate becomes

$$\alpha_{pk} = g(y)4\pi\frac{\gamma b_2^2 k_p^2}{MS\rho\omega_{pk}}\frac{a^3}{(2\pi)^3}\int d\vec{k}(u_{mk}v_{mk})^2 n_k^0\varepsilon_k \times \delta(\omega_{mk1} - \omega_{pk} - \omega_{mk2}), \quad (73)$$

which, with Eq. (71), can be written as

$$\alpha_{pk}(y) = \delta n_m(y)4\pi\frac{\gamma b_2^2 k_p^2 a^3}{MS\rho\omega_{pk}}\frac{I_{uv}}{I_0}, \quad (74)$$

where the integral I_{uv} is given by

$$I_{uv} = \frac{1}{(2\pi)^3}\int d\vec{k}(u_{mk}v_{mk})^2 n_k^0\varepsilon_k\delta(\omega_{mk1} - \omega_{pk} - \omega_{mk2}). \quad (75)$$

Using the relation between the magnon accumulation and the spin current, Eq. (47), and considering $t_{\rm FMI} \ll l_m$, we have

$$\delta n_m(y) \approx J_S\frac{l_m^2}{\hbar D_m t_{\rm FMI}}, \quad (76)$$

that replaced in Eq. (74) gives a direct relation between the pumping rate and the spin current:

$$\alpha_{pk} = J_S\frac{4\pi l_m^2}{\hbar D_m t_{\rm FMI}}\frac{\gamma b_2^2 k_p^2 a^3}{MS\rho\omega_{pk}}\frac{I_{uv}}{I_0}. \quad (77)$$

Finally, with Eq. (30) we obtain an expression for the pumping rate in terms of the charge current density, that replaced in Eq. (69) gives for the critical intensity of the charge current in the NM strip for phonon pumping

$$I_{cr} = \eta_{kp}\frac{et_{\rm FMI}wt_{\rm NM}}{2\pi\theta_{\rm SH}\tau_{mp}}\frac{MS\rho\omega_{pk}}{\gamma b_2^2 k_p^2 a^3}\frac{I_0}{I_{uv}}, \quad (78)$$

where w is the width of the NM strip and $\tau_{mp} = l_m^2/D_m$ is the magnon-phonon decay time.

IV. COMPARISON OF THEORY WITH EXPERIMENTS

A. Critical current for phonon pumping

For the calculation of the integrals in Eqs. (72) and (75), we introduce the dimensionless energy $x = \hbar\omega_k/k_BT$ and the normalized wave number $q = k/k_m$, where k_m is the radius of the Brillouin zone boundary, assumed to be spherical. Thus, the two integrals become

$$I_0 = \frac{k_BTk_m^3}{2\pi^2}\int_0^1 dqq^2\frac{x}{e^x - 1}, \quad (79)$$

$$I_{uv} = \frac{k_BTk_m^3}{2\pi^2}\int_0^1 dqq^2(u_{mq}v_{mq})^2\frac{x}{e^x - 1}\delta(\omega_{mk1} - \omega_{pk} - \omega_{mk2}). \quad (80)$$

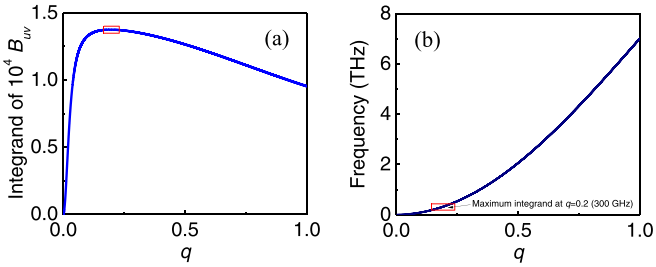

FIG. 5. (a) Plot of the integrand of B_{uv} in Eq. (81) versus normalized wave number showing that the maximum contribution is due to magnons with $q = 0.2$. (b) Magnon dispersion relation showing that magnons with $q = 0.2$ have frequency 300 GHz.

In the evaluation of I_{uv} we consider the representation for the delta function:

$$2\pi i\delta(\omega) = \lim_{\eta\to 0}\left(\frac{1}{\omega - i\eta} - \frac{1}{\omega + i\eta}\right) = \lim_{\eta\to 0}\left(\frac{2i\eta}{\omega^2 + \eta^2}\right). \tag{81}$$

Thus, since the energy conservation is satisfied for any value of ω_{pk}, in the integration we simply replace

$$\delta(\omega_{mk1} - \omega_{pk} - \omega_{mk2}) \to \frac{1}{\pi\eta_{mk1}}. \tag{82}$$

As we shall show later, we can assume that the magnons responsible for the pumping process are confined to a small region in the Brillouin zone, so that we can consider that the magnon relaxation rate $\eta_{mk1} \sim \eta_{m1}$ does not depend on k. Therefore, finally, since the two integrals have the same prefactor, that cancels out in the ratio, the critical current in Eq. (78) becomes

$$I_{cr} = \eta_{kp}\eta_{m1}\frac{et_{\rm FMI}wt_{\rm NM}}{2\theta_{\rm SH}\tau_{mp}}\frac{MS\rho\omega_{pk}}{\gamma b_2^2 k_p^2 a^3}\frac{B_0}{B_{uv}}, \tag{83}$$

where B_0 and B_{uv} are two dimensionless integrals given by

$$B_0 = \int_0^1 dqq^2\frac{x}{e^x - 1}, \tag{84}$$

$$B_{uv} = \int_0^1 dqq^2(u_{mq}v_{mq})^2\frac{x}{e^x - 1}. \tag{85}$$

The two integrals in (84) and (85) are easily integrated numerically, so that the critical current can be calculated with the known material parameters. Since the magnon relaxation rate η_{mk1} and the magnon-phonon decay time τ_{mp} depend on the magnon wave number, we need first to find the range of k_1 that dominates in the pumping process. Figure 5(a) shows the integrand of B_{uv} calculated numerically for YIG with the dispersion relation

$$\omega_k = \omega_{\rm ZB}\left(1 - \cos\frac{\pi q}{2}\right), \tag{86}$$

that best fits the measured dispersion of the acoustic magnons with $\omega_{\rm ZB} = 2\pi \times 7 \times 10^{12}\,{\rm s}^{-1}$ [43,44]. The values of the integrals (84) and (85) calculated numerically are $B_0 = 0.23$ and $B_{uv} = 1.2 \times 10^{-4}$.

Since the phonon pumping rate is proportional to the integral B_{uv}, one can consider that the magnons in the spin current that are most important in the pumping process are those in the region where the integrand of B_{uv} has maximum amplitude, which, as can be seen in Fig. 5(a), corresponds to a normalized wave number $q \approx 0.2$. Figure 5(b) shows that these magnons have frequency $\approx$ 300 GHz. Thus, in a first approximation, we can consider in Eq. (83) the values of η_{m1} and and τ_{mp} for $q = 0.2$. For the magnon relaxation rate we use the value calculated with four-magnon relaxation for $q = 0.2$, $\eta_{m1} = 5 \times 10^9\,{\rm s}^{-1}$ [44], and for the magnon-phonon decay time we use the value $\tau_{mp} = 10^{-8}$ s, which is intermediate between the values measured at low k [45,46] and high k [47]. The other sample and YIG material parameters are $t_{\rm NM} = 9 \times 10^{-7}$ cm, $w = 150\,\mu$m, $M = 140$ G, $t_{\rm FMI} = 1.54 \times 10^{-5}$ cm, $b_2 = 7.0 \times 10^6\,{\rm erg/cm}^3$, $\rho = 5.2\,{\rm g/cm}^3$, $a = 1.24 \times 10^{-7}$ cm, $S = 20$, $\gamma = 1.76 \times 10^7\,{\rm s}^{-1}$, $\theta_{\rm SH} = 0.45$, $\omega_{pk} = 2\pi \times 7.8 \times 10^9\,{\rm s}^{-1}$, $\eta_{pk} \approx 10^5\,{\rm s}^{-1}$ [48], and $k = \omega_{pk}/v_{pk} = 1.26 \times 10^5\,{\rm cm}^{-1}$. With these parameters, straightforward calculation of Eq. (83) gives for the critical current for phonon pumping $I_{cr} = 88$ mA. This value is in good order of magnitude agreement with the one measured in the BLS experiments [26].

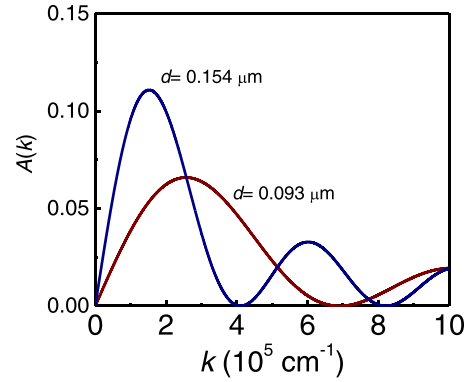

FIG. 6. Fourier transforms of the magnon accumulation in the YIG films with thicknesses $d = 154$ nm and $d = 93$ nm.

B. Frequency of the pumped phonons

The frequency of the pumped phonons depends on the conditions of the driving. Since the magnon-phonon-magnon process is proportional to the magnon accumulation, the driving is confined to region $0 \leqslant y \leqslant t_{\rm FMI} = d$. However, the phonons driven by the magnons in the spin current propagate into the GGG substrate and form standing waves between the outer YIG and GGG surfaces. We consider that the phonons that are driven with the largest intensity have a wave number that corresponds to the maximum of the Fourier transform of the driving. Figure 6 shows the Fourier transform $A(k)$ of the magnon accumulation in Fig. 3, calculated for YIG film thicknesses 154 and 93 nm, as in the experiments of Ref. [26]. In the calculation we have considered a magnon diffusion length $l_m = 1.0\,\mu$m, which is intermediate between the values measured in thin and thick films [15,43,44]. For $d = 154$ nm the wave number for the peak intensity is $k_p = 1.5 \times 10^5\,{\rm cm}^{-1}$. The corresponding wavelength is $\lambda = 2\pi/k_p = 418$ nm, such that $\lambda \approx 3\,d$. For $d = 93$ nm the wave number for the peak intensity is $k_p = 2.6 \times 10^5\,{\rm cm}^{-1}$,

corresponding to $\lambda = 242$ nm, such that again $\lambda \approx 3\,d$. Using for YIG $v_t = 3.84 \times 10^3$ m/s, we obtain from the relation $\lambda \approx 3\,d$ the frequencies 8.3 and 13.9 GHz for the films with thicknesses 154 and 93 nm, respectively, which are close to the measured values.

V. CONCLUSION

In conclusion, we have presented a theoretical formulation for phonon pumping by magnonic spin currents recently observed experimentally. This process is the Onsager reciprocal effect of the spin pumping by coherent elastic waves experimentally demonstrated several years ago. The experiments were performed with samples made of a YIG film with a metallic strip made of a platinum strip with nanoscopic silver particles that has been shown to have a giant spin Hall effect. An electric current injected in the metallic strip generates a spin current by means of the spin Hall effect that flows into the YIG film in the form of a magnonic spin current. Brillouin light scattering measurements demonstrate that for currents above a critical value, a peak shows up with a frequency in the microwave range that does not change with the applied magnetic field intensity but depends on the YIG film thickness. Here we have shown that the magnons in the spin current generate phonons by a three-boson process in which one magnon produces one phonon and one magnon by means of the magnetoelastic interaction. If the current intensity is larger than a critical value for which the phonon pumping rate overcomes the phonon damping, phonons with a certain frequency in the microwave range are excited. The critical current intensity and the frequency of the driven phonons calculated with the theory are in good agreement with the values measured experimentally. From a fundamental physics point of view, our results represent an important step in the research of the interconversion of phononic and spin degrees of freedom. Our findings also might provide an additional boost in the development of spintronic devices for information and communication technologies.

ACKNOWLEDGMENTS

The authors acknowledge helpful discussions with Antonio Azevedo. This research was supported by Conselho Nacional de Desenvolvimento Científico e Tecnológico (CNPq), Coordenação de Aperfeiçoamento de Pessoal de Nível Superior (CAPES), Financiadora de Estudos e Projetos (FINEP), and Fundação de Amparo à Ciência e Tecnologia do Estado de Pernambuco (FACEPE).

[1] J. R. Eshbach, Spin-Wave Propagation and the Magnetoelastic Interaction in Yttrium Iron Garnet, Phys. Rev. Lett. **8**, 357 (1962).

[2] W. Strauss, Magnetoelastic waves in yttrium iron garnet, J. Appl. Phys. **36**, 118 (1965).

[3] A. A. Auld, J. H. Collins, and D. C. Webb, Excitation of magnetoelastic waves in YIG delay lines, J. Appl. Phys. **39**, 1598 (1968).

[4] S. M. Rezende and F. R. Morgenthaler, Magnetoelastic waves in time-varying magnetic fields. I. Theory, J. Appl. Phys. **40**, 524 (1969).

[5] A. A. Serga, A. V. Chumak, and B. Hillebrands, YIG magnonics, J. Phys. D: Appl. Phys. **43**, 264002 (2010).

[6] A. V. Chumak, V. I. Vasyuchka, A. A. Serga, and B. Hillebrands, Magnon spintronics, Nat. Phys. **11**, 453 (2015).

[7] K. Uchida, H. Adachi, T. An, T. Ota, M. Toda, B. Hillebrands, S. Maekawa, and E. Saitoh, Long-range spin Seebeck effect and acoustic spin pumping, Nat. Mater. **10**, 737 (2011).

[8] M. Weiler, H. Huebl, F. S. Goerg, F. D. Czeschka, R. Gross, and S. T. B. Goennenwein, Spin Pumping with Coherent Elastic Waves, Phys. Rev. Lett. **108**, 176601 (2012).

[9] A. V. Azovtsev and N. A. Pertsev, Magnetization dynamics and spin pumping induced by standing elastic waves, Phys. Rev. B **94**, 184401 (2016).

[10] J. Puebla, M. Xu, B. Rana, K. Yamamoto, S. Maekawa, and Y. Otani, Acoustic ferromagnetic resonance and spin pumping induced by surface acoustic waves, J. Phys. D: Appl. Phys. **53**, 264002 (2020).

[11] A. Kamra, H. Keshtgar, P. Yan, and G. E. W. Bauer, Coherent elastic excitation of spin waves, Phys. Rev. B **91**, 104409 (2015).

[12] X. Li, D. Labanowski, S. Salahuddin, and C. S. Lynch, Spin wave generation by surface acoustic waves, J. Appl. Phys. **122**, 043904 (2017).

[13] T. Kikkawa, K. Shen, B. Flebus, R. A. Duine, K.-i. Uchida, Z. Qiu, G. E. W. Bauer, and E. Saitoh, Magnon Polarons in the Spin Seebeck Effect, Phys. Rev. Lett. **117**, 207203 (2016).

[14] B. Flebus, K. Shen, T. Kikkawa, K.-i. Uchida, Z. Qiu, E. Saitoh, R. A. Duine, and G. E. W. Bauer, Magnon-polaron transport in magnetic insulators, Phys. Rev. B **95**, 144420 (2017).

[15] L. J. Cornelissen, K. Oyanagi, T. Kikkawa, Z. Qiu, T. Kuschel, G. E. W. Bauer, B. J. van Wees, and E. Saitoh, Nonlocal magnon-polaron transport in yttrium iron garnet, Phys. Rev. B **96**, 104441 (2017).

[16] S. Streib, H. Keshtgar, and G. E. W. Bauer, Damping of Magnetization Dynamics by Phonon Pumping, Phys. Rev. Lett. **121**, 027202 (2018).

[17] K. An, A. N. Litvinenko, R. Kohno, A. A. Fuad, V. V. Naletov, L. Vila, U. Ebels, G. de Loubens, H. Hurdequint, N. Beaulieu, J. Ben Youssef, N. Vukadinovic, G. E. W. Bauer, A. N. Slavin, V. S. Tiberkevich, and O. Klein, Coherent long-range transfer of angular momentum between magnon Kittel modes by phonons, Phys. Rev. B **101**, 060407(R) (2020).

[18] A. Rückriegel and R. A. Duine, Long-Range Phonon Spin Transport in Ferromagnet–Nonmagnetic Insulator Heterostructures, Phys. Rev. Lett. **124**, 117201 (2020).

[19] C. Zhao, Y. Li, Z. Zhang, M. Vogel, J. E. Pearson, J. Wang, W. Zhang, V. Novosad, Q. Liu, and A. Hoffmann, Phonon Transport Controlled by Ferromagnetic Resonance, Phys. Rev. Appl. **13**, 054032 (2020).

[20] H. Man, Z. Shi, G. Xu, Y. Xu, X. Chen, S. Sullivan, J. Zhou, K. Xia, J. Shi, and P. Dai, Direct observation of magnon-phonon coupling in yttrium iron garnet, Phys. Rev. B **96**, 100406(R) (2017).

[21] J. Holanda, D. S. Maior, A. Azevedo, and S. M. Rezende, Detecting the phonon spin in magnon-phonon conversion experiments, Nat. Phys. **14**, 500 (2018).

[22] L. Chotorlishvili, X.-G. Wang, Z. Toklikishvili, and J. Berakdar, Thermoelastic enhancement of the magnonic spin Seebeck effect, Phys. Rev. B **97**, 144409 (2018).

[23] N. Ogawa, W. Koshibae, A. J. Beekman, N. Nagaosa, M. Kubota, M. Kawasaki, and Y. Tokura, Photodrive of magnetic bubbles via magnetoelastic waves, Proc. Natl. Acad. Sci. USA **112**, 8977 (2015).

[24] K. An, K. S. Olsson, A. Weathers, S. Sullivan, X. Chen, X. Li, L. G. Marshall, X. Ma, N. Klimovich, J. Zhou, L. Shi, and X. Li, Magnons and Phonons Optically Driven out of Local Equilibrium in a Magnetic Insulator, Phys. Rev. Lett. **117**, 107202 (2016).

[25] D. A. Bozhko, P. Clausen, G. A. Melkov, V. S. L'vov, A. Pomyalov, V. I. Vasyuchka, A. V. Chumak, B. Hillebrands, and A. A. Serga, Bottleneck Accumulation of Hybrid Magnetoelastic Bosons, Phys. Rev. Lett. **118**, 237201 (2017).

[26] J. Holanda, D. S. Maior, O. Alves Santos, A. Azevedo, and S. M. Rezende, Evidence of phonon pumping by magnonic spin currents, Appl. Phys. Lett. **118**, 022409 (2021).

[27] O. Alves-Santos, E. F. Silva, M. Gamino, R. O. Cunha, J. B. S. Mendes, R. L. Rodríguez-Suárez, S. M. Rezende, and A. Azevedo, Giant spin-charge conversion driven by nanoscopic particles of Ag in Pt, Phys. Rev. B **96**, 060408(R) (2017).

[28] N. Zagury and S. M. Rezende, Theory of macroscopic excitations of magnons, Phys. Rev. B **4**, 201 (1971).

[29] S. M. Rezende, *Fundamentals of Magnonics*, Lecture Notes in Physics Vol. 969 (Springer, Cham, Switzerland, 2020).

[30] C. Kittel, Interaction of spin waves and ultrasonic waves in ferromagnetic crystals, Phys. Rev. **110**, 836 (1958).

[31] E. Schlömann and R. I. Joseph, Generation of spin waves in nonuniform magnetic fields. III. Magnetoelastic interaction, J. Appl. Phys. **35**, 2382 (1964).

[32] A. I. Akhiezer, V. G. Bar'yakhtar, and S. V. Peletminskii, *Spin Waves* (North-Holland, Amsterdam, 1968).

[33] A. G. Gurevich and G. A. Melkov, *Magnetization Oscillations and Waves* (CRC, Boca Raton, FL, 1994).

[34] A. Rückriegel, P. Kopietz, D. A. Bozhko, A. A. Serga, and B. Hillebrands, Magnetoelastic modes and lifetime of magnons in thin yttrium iron garnet films, Phys. Rev. B **89**, 184413 (2014).

[35] S. C. Guerreiro and S. M. Rezende, Magnon-phonon interconversion in a dynamically reconfigurable magnetic material, Phys. Rev. B **92**, 214437 (2015).

[36] J. E. Hirsch, Spin Hall Effect, Phys. Rev. Lett. **83**, 1834 (1999).

[37] A. Hoffmann, Spin Hall effects in metals, IEEE Trans. Magn. **49**, 5172 (2013).

[38] S. Maekawa, H. A. Adachi, K. Uchida, J. Ieda, and E. Saitoh, Spin current: Experimental and theoretical aspects, J. Phys. Soc. Jpn. **82**, 102002 (2013).

[39] J. Sinova, S. O. Valenzuela, J. Wunderlich, C. H. Back, and T. Jungwirth, Spin Hall effects, Rev. Mod. Phys. **87**, 1213 (2015).

[40] *Spin Current*, 2nd ed., edited by S. Maekawa, S. O. Valenzuela, E. Saitoh, and T. Kimura (Oxford University Press, Oxford, 2017).

[41] S. S.-L. Zhang and S. Zhang, Magnon Mediated Electric Current Drag Across a Ferromagnetic Insulator Layer, Phys. Rev. Lett. **109**, 096603 (2012).

[42] S. S.-L. Zhang and S. Zhang, Spin convertance at magnetic interfaces, Phys. Rev. B **86**, 214424 (2012).

[43] S. M. Rezende, R. L. Rodríguez-Suárez, R. O. Cunha, A. R. Rodrigues, F. L. A. Machado, G. A. Fonseca Guerra, J. C. López Ortiz, and A. Azevedo, Bulk magnon spin current theory for the longitudinal spin Seebeck effect, Phys. Rev. B **89**, 014416 (2014).

[44] S. M. Rezende, R. L. Rodríguez-Suárez, J. C. López Ortiz, and A. Azevedo, J. Magn. Magn. Mater. **400**, 171 (2016).

[45] M. Sparks, Theory of three-magnon ferromagnetic relaxation frequency for low temperatures and small wave vectors, Phys. Rev. **160**, 364 (1967).

[46] S. O. Demokritov, V. E. Demidov, O. Dzyapko, G. A. Melkov, A. A. Serga, B. Hillebrands, and A. N. Slavin, Bose–Einstein condensation of quasi-equilibrium magnons at room temperature under pumping, Nature **443**, 430 (2006).

[47] J. S. Jamison, Z. Yang, B. L. Giles, J. T. Brangham, G. Wu, P. C. Hammel, F. Yang, and R. C. Myers, Long lifetime of thermally excited magnons in bulk yttrium iron garnet, Phys. Rev. B **100**, 134402 (2019).

[48] S. M. Rezende and F. R. Morgenthaler, Magnetoelastic waves in time-varying magnetic fields. II. Experiments, J. Appl. Phys. **40**, 537 (1969).